Received: 6 November 2015 | Revised: 23 May 2016 | Accepted: 10 July 2016

DOI 10.1002/etep.2255

WILEY

RESEARCH ARTICLE

A comparative validation of a synchronous generator by trajectory sensitivity and offline methods

Lucas Beordo | Elmer P. T. Cari | Taylon G. Landgraf | Luis F. C. Alberto

Department of Electrical Engineering, University of São Paulo (EESC/USP), Avenida Trabalhador São-carlense 400, 13566-590 São Carlos / SP, Brazil

Correspondence
Lucas Beordo, Department of Electrical Engineering, University of São Paulo (EESC/USP), Avenida Trabalhador São Carlense 400, 13566–590 - São Carlos / SP, Brazil
Email: beordo@usp.br

Summary

This paper addresses a comparison between *online* and *offline* methods to estimate parameters of a synchronous generator. The main aim of this comparison is to validate the results of a new *online* method based on trajectory sensitivity method against *offline* method. Steady-state, sudden short circuit, and voltage recovery tests were selected among the *offline* methods to serve of comparison for trajectory sensitivity method. The online method has the following features: It uses only terminal voltages and currents and field voltage measurements, it does not need the power angle, and it estimates the power angle using an auxiliary algebraic equation. Tests were conducted in a 2-kVA salient pole machine, and the differences in parameter values obtained from each approaches were analyzed. Eventually, it is concluded that technique based on trajectory sensitivity provides more reliable generator parameters of estimation process.

KEYWORDS

electric power system, offline test, parameter estimation, synchronous generator, trajectory sensitivity, validation

1 | INTRODUCTION

1.1 | Motivation

Computer-aided analysis is commonly used by engineers to ensure a safe and efficient operation of power systems. Given the importance of synchronous generators for electricity supply, the correct representation of these machines in these analyses is crucial, and the estimation of generator parameters is mandatory for model validation.

Techniques for parameter estimation are very common in different applications, such as wind turbines,[1] excitation systems,[2] induction motors,[3,4] and load models.[5,6]

The literature reports several methods for the determination of parameters of synchronous machines, which can be mainly classified into *offline* and *online* methods.

O*ffline* methods are applied when the machine is out of operation and can be classified into frequency domain and time domain methods. Among the offline methods based on time domain, the more traditional method are the steady-state test,[7] sudden short circuit (SSC) test,[8] voltage recovery test, and load rejection test. IEEE has standardized many of these approaches.[9] Usually, these procedures involve difficult and time consuming during the execution of the tests and are executed in specific operation condition.

For the shortcomings of *offline* methods to be overcome, the *online* methods to determine parameters with the machine connected in the grid have been proposed.[10–13]

New online approaches such as using an observer from neural networks and Prony method can be found in Shafighi et al,[14] Shariati et al,[15] and Deghani and Nikravesh,[16] respectively. In addition in Karayaka et al[17] the generator parameters are estimated using operating data. In all those researches[14-17] the availability of power angle measurement is necessary to estimate the parameter, which is not always possible in practice.

1.2 | Contribution

This paper presents an experimental validation of generator by *online* method based on trajectory sensitivity, and the results are compared with some standard *offline* methods. The proposed method has many good features such as follows:

 Copyright © 2016 John Wiley & Sons, Ltd.

20507038, 2017, 2, Downloaded from https://onlinelibrary.wiley.com/doi/10.1002/etep.2255 by Univ of Sao Paulo - Brazil, Wiley Online Library on [10/01/2023]. See the Terms and Conditions (https://onlinelibrary.wiley.com/terms-and-conditions) on Wiley Online Library for rules of use; OA articles are governed by the applicable Creative Commons License

it uses only measurements that are ease to obtain in the practice (terminal voltage and current, and field voltage), it does not need the power angle, it includes an algebraic equation in the model, and as a consequence, the power angle is estimated. This paper is a continuation of the work presented in Cari and Alberto[18] where the generator parameters were estimated using only simulation results. In this paper the generator parameters are validated using real measurements, and a comparison with *offline* methods are accomplished.

1.3 | Organization of the paper

This paper is organized as follows: Section 2 introduces the trajectory sensitivity method to determine parameters of nonlinear dynamic system and its application for synchronous generators. Section 3 show the estimation results from trajectory sensitivity method and some standards *offline* methods. Section 4 presents the comparison of results between trajectory sensitivity and *offline* methods. Section 5 provides the conclusions.

2 | ESTIMATION OF GENERATOR PARAMETERS BY TRAJECTORY SENSITIVITY METHOD

2.1 | Trajectory sensitivity method for estimation parameters of nonlinear system

Trajectory sensitivity method has been recently used in different application in electric power systems,[19,20] In this method the output variation regarded to parameter variation is called "sensitivity," and that information is used to update the parameter of the model.

Consider the nonlinear model

$$\begin{aligned}\frac{d}{dt}x(t) &= f(x(t),z(t),p,u(t))\\ 0 &= g(x(t),p,u(t))\\ y &= h(x(t),z(t),p,u(t))\end{aligned} \tag{1}$$

where x is the vector of the state variables, y is the vector of the system outputs, u is the input vector, p is the parameter vector to be determined, and f, g, and h are nonlinear continuous functions of x, p, and u, respectively. Let p_i be the ith component of vector p and f, g *and* h differentiable with respect to parameters p_i of p.

The sensibility functions are obtained by differentiating equations (1) in relation to parameters p_i

$$\frac{d}{dt}\frac{\partial x}{\partial p_i} = \frac{\partial f(x,z,p,u)}{\partial x}\cdot\frac{\partial x}{\partial p_i} + \frac{\partial f(x,z,p,u)}{\partial z}\cdot\frac{\partial z}{\partial p_i} + \frac{\partial f(x,z,p,u)}{\partial p_i}$$

$$0 = \frac{\partial g(x,z,p,u)}{\partial x}\cdot\frac{\partial x}{\partial p_i} + \frac{\partial g(x,z,p,u)}{\partial z}\frac{\partial z}{\partial p_i} + \frac{\partial f(x,z,p,u)}{\partial p_i} \tag{2}$$

$$\frac{\partial y}{\partial p_i} = \frac{\partial h(x,z,p,u)}{\partial x}\cdot\frac{\partial x}{\partial p_i} + \frac{\partial h(x,z,p,u)}{\partial z}\frac{\partial z}{\partial p_i} + \frac{\partial h(x,z,p,u)}{\partial p_i}$$

The parameters can be estimated by the solution of the optimization problem given by

$$J(p) = \frac{1}{2}\int_0^T (y_{med}(t)-y(t))^T(y_{med}(t)-y(t))dt \tag{3}$$

where y_{med} is the output vector of the measured values and y is the system's output vector. The optimality condition $\frac{\partial J(p)}{\partial p} = 0$ is denoted by

$$G(p) = \frac{\partial J(p)}{\partial p} = -\int_0^T \left(\frac{\partial y}{\partial p}\right)^T (y_{med}-y)dt = 0 \tag{4}$$

Newton's Raphson method can be used to solve (4) by iterative procedure given by

$$p^{(k+1)} = p^k - h_{opt}\Gamma\left(p^k\right)^{-1}G\left(p^k\right) \tag{5}$$

where h_{opt} is an optimum step and $\Gamma(p)$ is the Jacobian matrix of $G(p)$. More details about the procedure can be found in Cari and Alberto.[18]

2.2 | Generator modeling

The original equation of the 1-axis model valid for a salient pole rotor was rewritten for the estimation of the parameter from accessible measurements

$$\begin{aligned}\dot{E}'_q &= \tfrac{1}{T'_{do}}\left[\tfrac{V_f}{C} - E'_q + \left(X_d - X'_d\right)I_d\right]\\ 0 &= \mathrm{I}_\mathrm{T}^2 - \mathrm{I}_\mathrm{q}^2 - \mathrm{I}_\mathrm{d}^2\end{aligned}$$

$$P_e = E'_q I_q + \left(X'_d - X'_q\right)I_d I_q \tag{6}$$

$$\begin{aligned}Q_e &= -E'_q I_d - X'_q I_q^2 - X'_q I_d^2\\ I_d &= \tfrac{1}{X'_d}\left(U_T\cos(\beta) - E'_q\right)\\ I_q &= \tfrac{1}{X'_q}\left(U_T\,\mathrm{sen}(\beta)\right)\end{aligned}$$

where C is a proportional factor that relates excitation voltage ($\mathrm{E_{fd}}$) to field voltage (V_f) through the next relationship $E_{fd} = \frac{V_f}{C}$. The model represented by (6) contains one state variable $x = \left[\, E'_q(t)\right]$, one algebraic variable $z = [\,\beta(t)]$ (power angle or load angle), and six parameters $p = \left[X_d, X'_d, T'_{do}, X'_q, \mathrm{C}, E'_{qo}\right]^T$ (the initial condition of state variable, E'_{qo}, was also considered parameter). The input vector is $u = (\, U_T(t), I_T(t), \mathrm{V}_f(t)\,)$ and the output vector is $y = (\, P_e(t), Q_e(t)\,)$. The parameters of the generator are estimated by the procedure described in Section 2.1. Eventually, for a salient pole generator, X_q is assumed equal to X'_q.

3 | RESULTS AND DISCUSSIONS

A 2-kVA salient pole synchronous machine in Y configuration was used for parameter estimation and validation of

20507038, 2017, 2, Downloaded from https://onlinelibrary.wiley.com/doi/10.1002/etep.2255 by Univ of Sao Paulo - Brazil, Wiley Online Library on [10/01/2023]. See the Terms and Conditions (https://onlinelibrary.wiley.com/terms-and-conditions) on Wiley Online Library for rules of use; OA articles are governed by the applicable Creative Commons License

method based on sensitivity of trajectory analysis. The summary of the generator nameplate is shown in Table 1.

The nameplate generator data were used as base values (S_b = 2000 [VA] and V_b = 220 [V]) and impedance, and current base was determined Z_b = 24.2 [Ω] and I = 5.24 [A], respectively.

3.1 | Parameters estimation from trajectory sensitivity method

A small power system (Figure 1) was designed at the electrical engineering laboratory of Sao Paulo University for the obtaining of the measurement data by the online method.

The system is composed of a synchronous generator, a transmission line (impedance), and 2 loads. Initially, the generator provided power to a resistive load. A dynamic load composed of a resistors bank in parallel with a capacitors bank and a 3-phase induction motor was added at time 0.5 s.

The 3-phase terminal voltages and currents and the field voltage were sampled by LabVIEW software. The measurements were transformed into p.u. with the nominal values of the generator base. The voltages and currents in positive sequence and power factor were obtained by Fortescue's transform, and the active and reactive power was calculated from these values.

The voltage profile in p.u. prior and after the application of the perturbation is shown in Figure 2.

The trajectory sensitivity method presented in Section 2 was used for the estimation of the parameters. Figures 3 and 4 compare the active power and Figures 5 and 6 compare the reactive power of the real system (Actual) and the mathematical model (Model) at the beginning of the process and after the convergence of the parameters, respectively. Eight iterations and 2 min, on average, were necessary for a computer of 3-GHz memory to reach convergence.

In spite of the generator model being approached (transient model), the main behavior of active and reactive

TABLE 1 Nameplate for the Synchronous Machine

Salient pole synchronous machine		
U_{rated}	220	V
$I_{armature}$	5	A
Rated power	2000	VA
I_{field} (max)	0.6	A
ω	1800	RPM
Power factor	0.8	

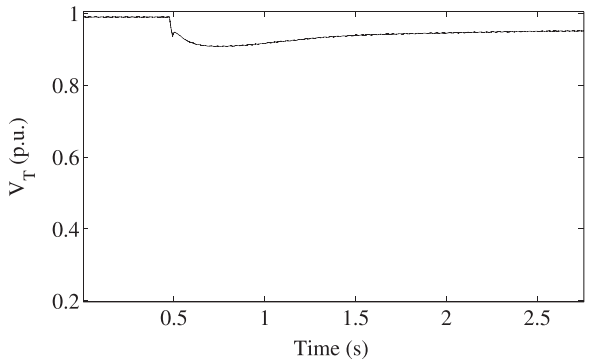

FIGURE 2 Terminal Voltage of Synchronous Generator

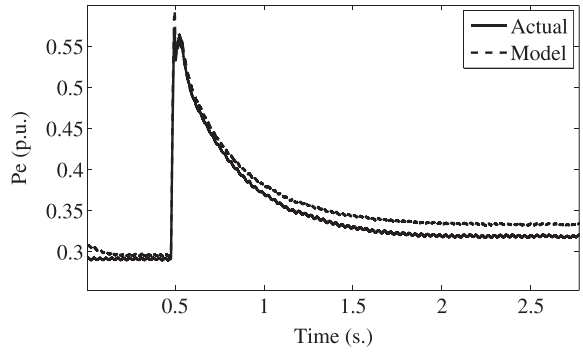

FIGURE 3 Active Power Before the Convergence of the Parameters

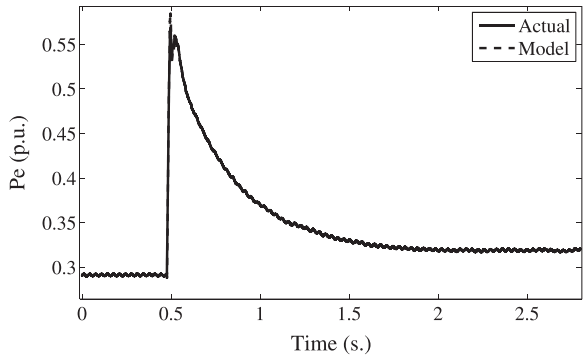

FIGURE 4 Active Power After the Convergence of the Parameters

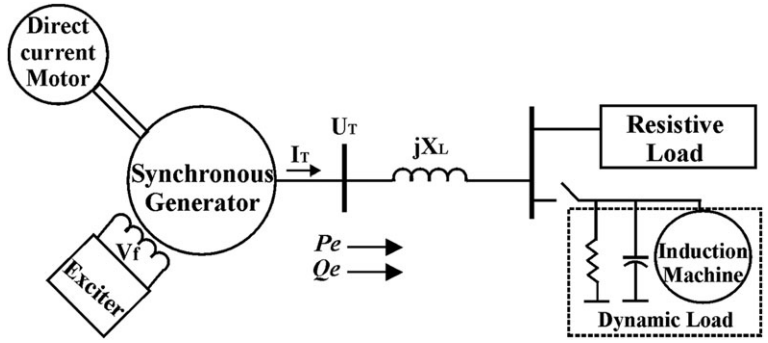

FIGURE 1 Framework for the Obtaining of the Measurement Data

20507038, 2017, 2, Downloaded from https://onlinelibrary.wiley.com/doi/10.1002/etep.2255 by Univ of Sao Paulo - Brazil, Wiley Online Library on [10/01/2023]. See the Terms and Conditions (https://onlinelibrary.wiley.com/terms-and-conditions) on Wiley Online Library for rules of use; OA articles are governed by the applicable Creative Commons License

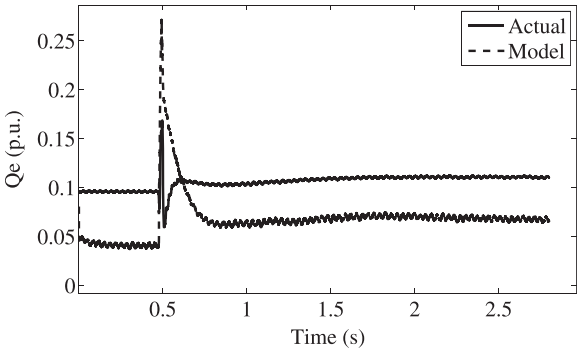

FIGURE 5 Reactive Power Before the Convergence of the Parameters

power was reached after the convergence of parameter (Figures 4 and 6).

Table 2 shows a result of trajectory sensivity method (online method).

After the application of the perturbation (inclusion of the dynamic load), the voltage changed to 115 V (line to neutral) or 0.90 p.u., as shown in Figure 2. Therefore, the *d*-axis reactance determined in Table II must be corrected to nominal value 127 V (line to neutral). A factor was obtained by the division of $k = 115/127$ or k = 0.9 for the determination of saturated *d*-axis reactance at nominal value as

$X_{ds} = X_d$ *k

$X_{ds} = 1.09$ p.u.

3.2 | Parameters estimation from offline methods

The parameters to be estimated will depend on the type of the test. In this study, steady-state, SSC, and opening short circuit tests were chosen. The procedure to execute those tests was according STD-IEEE.[9]

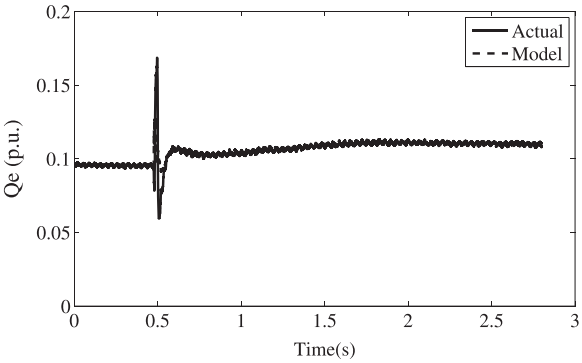

FIGURE 6 Reactive Power After the Convergence of the Parameters

TABLE 2 Online Method Results (Trajectory Sensitivity Method)

Parameters	Value (p.u.)
X_d (p.u.)	1.22
X'_d (p.u.)	0.49
X'_q (p.u.)	0.574
T'_{do}(s)	0.248
C (V)	83.07
E'_{qo} (p.u.)	1.046

3.2.1 | Steady-state tests

The direct and quadrature axis synchronous reactances (X_d and X_q, respectively) can be estimated by such tests.

3.2.2 | Tests using no-load saturation curve and short-circuit characteristic

These tests determine the saturated and unsaturated synchronous reactances of generator (X_{ds} and X_{du}, respectively).

The no-load saturation curve (NLSC) and short-circuit characteristic (SCC) for the 2-kVA machine is shown in Figure 7.

The synchronous reactances are given by

$$X_{ds} = \frac{U_{an}}{I_a} \tag{7}$$

$$X_{du} = \frac{U_{ae}}{I_a} \tag{8}$$

where U_{an} is the nominal generator voltage in the no-load operation curve, U_{ae} is the armature voltage in the air-gap line, and I_a is the armature current for the value of the field current obtained.

Figure 7 shows the NLSC (voltage line to neutral) curve, air-gap line and SCC (short circuit current multiplied by factor 10) for the machine tested.

For nominal voltage $U_{an} = 127$ V, the following results were founded.

$I_F = 0.331$ A; $I_a = 6.350$ A; $U_{ae} = 169.037$ V

The values of reactances were calculated by equations (7) and (8)

$X_{ds} = 20\ \Omega$

$X_{du} = 26.62\ \Omega$

The saturated and unsaturated *d*-axis reactances as a function of the terminal voltage obtained from the tests are

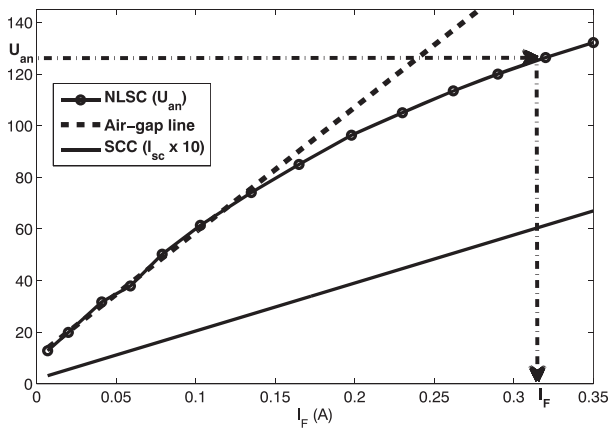

FIGURE 7 NLSC, SCC, and Air-gap Line. NLSC Indicates No-load Saturation Curve; SCC, Short Circuit Characteristic

20507038, 2017, 2, Downloaded from https://onlinelibrary.wiley.com/doi/10.1002/etep.2255 by Univ of Sao Paulo - Brazil, Wiley Online Library on [10/01/2023]. See the Terms and Conditions (https://onlinelibrary.wiley.com/terms-and-conditions) on Wiley Online Library for rules of use; OA articles are governed by the applicable Creative Commons License

shown in Figure 8. The values X_{ds} and X_{du} can be verified in Figure 8.

3.2.3 | Slip test

This test determines the saturated reactances of the direct axis (X_{ds}) and quadrature axis (X_{qs}). The generator is turned slightly differently from the synchronous speed with field windings in open circuit. An external 3-phase source variable must be connected to the generator armature terminals in the same phase sequence. However, the generator cannot be synchronized with the source. The armature voltage and current values must be analyzed. The induced field voltage can also be measured for a clear visualization of the minimum and maximum points of currents and voltages.

When the field voltage reaches its maximum value, the envelope of the armature voltage and current reaches their minimum and maximum peaks, respectively. The direct-axis reactance can be determined with these values. When the field voltage reaches its zero value, the envelope of the armature current and voltage reaches their minimum and maximum peaks, respectively. The reactances can be determined by

$$X_{qs} = \frac{U_{a\min}}{I_{a\max}} \tag{9}$$

$$X_{ds} = \frac{U_{a\max}}{I_{a\min}} \tag{10}$$

The slip test was applied to two different voltage levels, 52 and 180 V (Figures 9 and 10), for the obtaining of unsaturated and saturated values for the reactances, respectively.

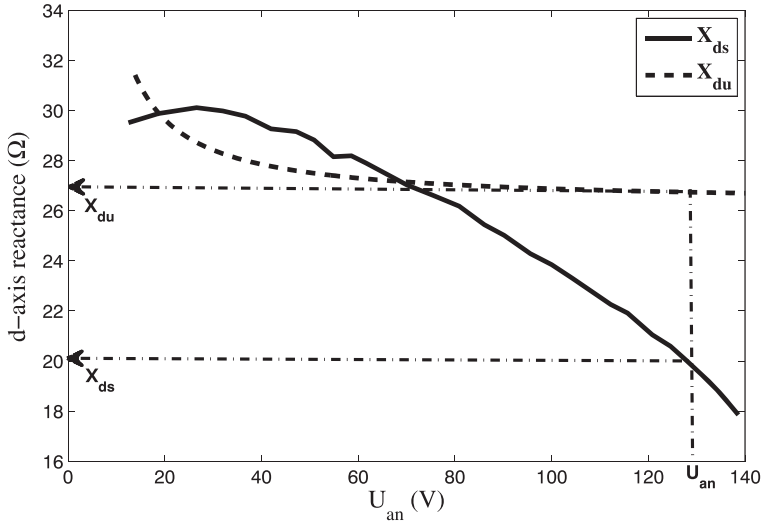

FIGURE 8 Synchronous Saturated and Unsaturated *d*-Axis Reactances

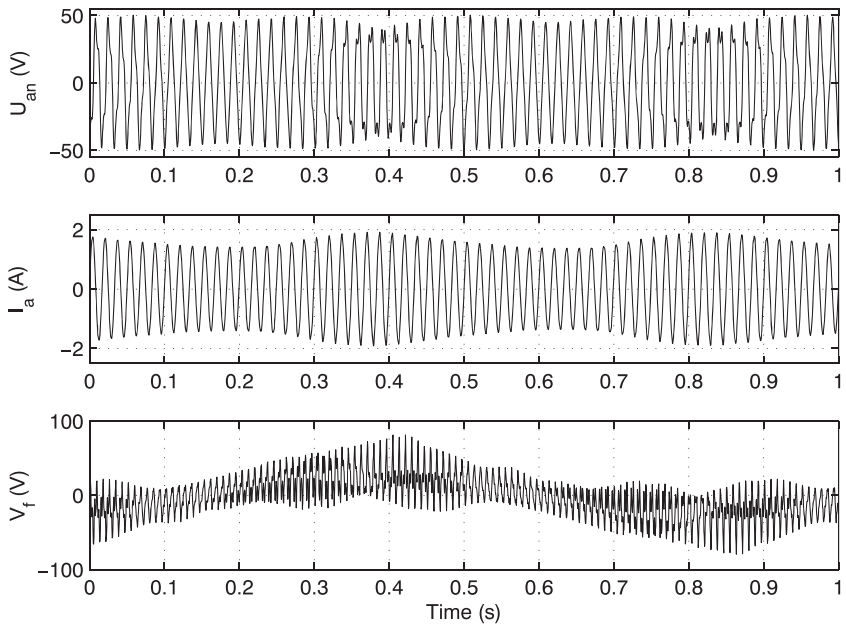

FIGURE 9 Slip Test at 52 V

20507038, 2017, 2, Downloaded from https://onlinelibrary.wiley.com/doi/10.1002/etep.2255 by Univ of Sao Paulo - Brazil, Wiley Online Library on [10/01/2023]. See the Terms and Conditions (https://onlinelibrary.wiley.com/terms-and-conditions) on Wiley Online Library for rules of use; OA articles are governed by the applicable Creative Commons License

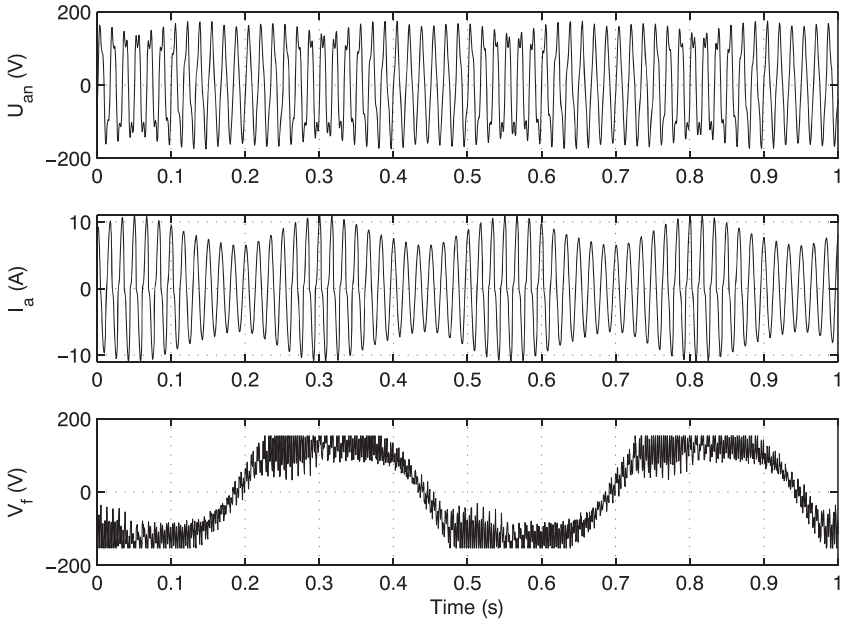

FIGURE 10 Slip Test at 180 V

The results for the slip test at 52 V were

$U_{a\_max} = 50.51$ V ; $I_{a\_min} = 1.64$ A; $U_{a\_min} = 40.13$ V ; $I_{a\_max} = 2.02$ A;

$X_{du} = 30.8\ \Omega$ $X_{qu} = 19.87\ \Omega$

And the results for the slip test at 180 V were

$U_{a\_max} = 171.7$ V ; $I_{a\_min} = 7.37$ A; $U_{a\_min} = 131.7$ V ; $I_{a\_max} = 11.53$ A;

$X_{ds} = 23.30\Omega$; $X_{qs} = 11.42\ \Omega$

3.2.4 | Maximum lagging current test

This test determines the saturated synchronous reactance in the quadrature axis (X_{qs}) of generators. The machine is operated as a motor with nonload and must be set at a synchronous speed. The field current is then decreased to zero and then increased with reverse polarity until it has produced instability. The voltage applied (U_{an}) and the current before instability (I_a) are registered, and the reactance is calculated by

$$X_{qs} = \frac{U_{an}}{I_a} \tag{11}$$

The maximum lagging test was performed at 220 V, and the saturate q-axis reactance obtained was $X_{qs} = 13.55\ \Omega$ (Figure 11).

3.2.5 | SSC test

The SSC test at the armature windings determines direct-axis generator parameters, such as synchronous, transient, and subtransient reactances ($X_d, X_d^{'}$, and $X_d^{''}$, respectively) and transient and sub-transient time constants ($T_d^{'}$ and $T_d^{''}$, respectively).

The generator is driven at a synchronous speed with the armature terminals in open circuit. The field winding is excited, so that some armature voltage is induced. At a certain instant the contact of the armature terminals is closed, which causes a 3-phase short circuit in the generator. The currents in the armature windings are acquired by a data acquisition system as shown in Figure 12. The procedure to determine the parameters from this test can be found in Appendix A.

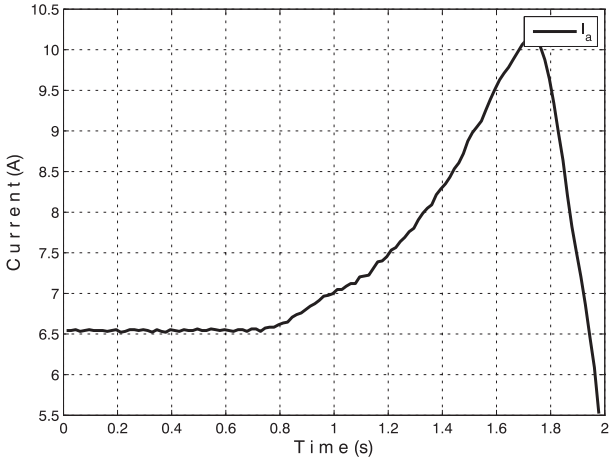

FIGURE 11 Maximum Lagging Current Test

The values obtained for this test were as follows: U = 78.30 [V]; I_{ss} = 2.37 [A]; $I^{'}$ = 8.25 [A]; $I^{''}$ = 16.81 [A], A = 10.63; B = 27.44; X_{du} = 33.04 [Ω]; $X_d^{'}$ = 7.37 [Ω]; $X_d^{''}$ = 2.86 [Ω]; $T_d^{'}$ = 0.0599 [s]; $T_d^{''}$ =0.0081 [s].

The comparison of current sampled (data) and obtained by equation is shown in Figure 13.

The SCC test was also accomplished at rated voltage (220 V); the values were the following:

U = 179.61 [V]; I_{ss} = 7.699 [A]; $I^{'}$ = 13.137 [A]; $I^{'}$ = 10.96 [A], A = 20.84; B = 31.78, X_{du} = 23.33 [Ω]; $X_d^{'}$ = 8.62 [Ω]; $X_d^{''}$ = 5.65 [Ω]; $T_d^{'}$ = 0.0581 [s]; $T_d^{''}$ = 0.0250 [s].

20507038, 2017, 2, Downloaded from https://onlinelibrary.wiley.com/doi/10.1002/etep.2255 by Univ of Sao Paulo - Brazil, Wiley Online Library on [10/01/2023]. See the Terms and Conditions (https://onlinelibrary.wiley.com/terms-and-conditions) on Wiley Online Library for rules of use; OA articles are governed by the applicable Creative Commons License

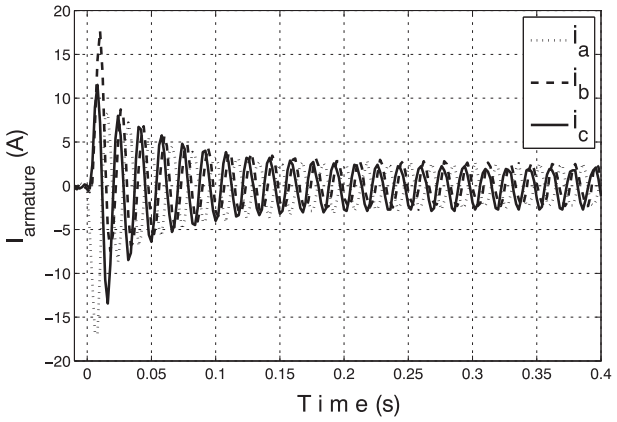

FIGURE 12 Sudden Short Circuit Test at 96.25 V

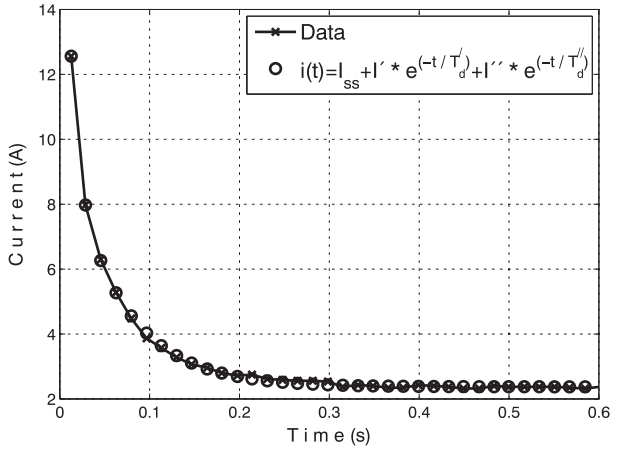

FIGURE 13 Comparison of Data and by Short Circuit Current Equation

3.2.6 | Voltage recovery test

This test can be performed through the opening of the generator terminals after a short circuit test, and the same reactances are obtained. The time constants, in this case, are open circuit transient and subtransient time constants (T'_{do} and T''_{do}, respectively).

Figure 14 shows the results of the test, and the procedure to determine the parameter can be found in Appendix B.

The values determined for this test were as follows: $U_{ao} = 174.46$ [V]; $U' = 65.83$ [A]; $U'' = 37.62$ [A]; $I_{sc} = 7.55$ [A]; $X_d = 23.10$ [Ω]; $X'_d = 8.72$ [Ω]; $X''_d = 4.98$ [Ω]; $T'_{do} = 0.2679$ [s]; $T''_{do} = 0.1858$ [s].

3.3 | Correction to specific temperature

Parameter T'_d and T'_{do} may be corrected because variation of rotor field resistance using similar formula proposed in Std 115-1995 (p. 134)[9]:

$$T'_d = T'_{dt}\left(\frac{k+t_t}{k+t_s}\right)$$

where T'_d is the direct-axis transient short circuit time constant at specific temperature; T'_{dt} is the direct-axis transient short circuit time constant at test temperature; t_t is the average temperature of the field winding during the test, °C; t_s is the specific temperature, °C; and k is the factor, depending on the current conducting material (k for copper is 234.5°).

In addition t_t may be determined by[9]

$$t_t = t_s + \left(\frac{R_t - R_s}{R_s}\right)(t_s + k)$$ where R_t is the resistance measured during the test and R_s is the resistance previously measured at known temperature t_s.

For our experiment, $t_s = 25$°C, $R_s = 230.5$°C, and $R_t = 243.5$°C. From those values, $t_t = 43.2$°C.

From SSC test at 96.25 V, $T'_{dt} = 0.0599$s ; then, the corrected value of T'_d was 0.0641.

From SSC test at 220 V, $T'_{dt} = 0.0581s$; then, the corrected value of T'_d was 0.0621.

Through the use of a similar procedure, T'_{do} may be corrected. From voltage recovery test at 220 V, $T'_{do} = 0.2679$s ; then, the corrected value of T'_d was 0.2866.

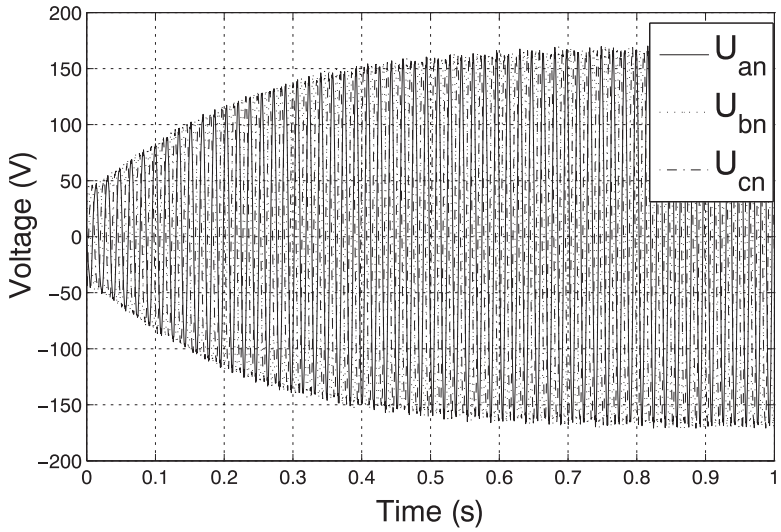

FIGURE 14 Voltage Recovery Test at 220 V

20507038, 2017, 2, Downloaded from https://onlinelibrary.wiley.com/doi/10.1002/etep.2255 by Univ of Sao Paulo - Brazil, Wiley Online Library on [10/01/2023]. See the Terms and Conditions (https://onlinelibrary.wiley.com/terms-and-conditions) on Wiley Online Library for rules of use; OA articles are governed by the applicable Creative Commons License

TABLE 3 Parameter Identified by Offline Tests in Per Unit

Paramaters	Steady-state test				Sudden short circuit test (96.25 V)	Sudden short circuit test (220 V)	Voltage recovery test (220 V)	Selected parameters*
	NLSC and SCC	Slip test (52 V)	Slip test (180 V)	MLC test (220 V)				
X_{du}	1.10	1.27			1.365*			1.365
X_{ds}	0.826		0.96			0.960*	0.955	0.960
$X_d^{'}$					0.305	0.360*	0.360	0.360
$X_d^{''}$					0.118	0.230*	0.2058	0.230
X_{qu}		0.82						0.82
X_{qs}			0.47	0.56*				0.56
$T_d^{'}$(s)					0.0641	0.0621*	0.1279©	0.0581
$T_d^{''}$(s)					0.0081	0.0250*	0.0725©	0.0250
$T_{do}^{'}$(s)					0.2869©	0.1682©	0.2866*	0.2866
$T_{do}^{''}$(s)					0.0209©	0.0391©	0.1858*	0.1858

Abbreviations: NLSC, no-load saturation curve; SCC, short circuit characteristic; MLC, maximum lagging current.

3.3.1 | Parameters compilation from offline tests

Table 3 summarizes the parameters obtained experimentally in the *offline* tests presented in this section. Reactances are in per unit ($Z_b = 24.2$ [Ω]) and time constants are given in seconds.

The following relationship $\frac{T_d^{'}}{T_{do}^{'}} = \frac{X_d^{'}}{X_d}$ and $\frac{T_d^{''}}{T_{do}^{''}} = \frac{X_d^{''}}{X_d^{'}}$ determines the open circuit time constant from the short circuit time constant and vice versa.[7] Those values were denoted for symbol © in Table 3.

Slip tests were conducted in 52 and 180 V (24% and 82% of the nominal voltage value); therefore, unsaturated and saturated reactances for X_d and X_q, respectively, were determined in each test.

The SSC test was set to 96.25 and 220 V; therefore, the reactance determined an unsaturated value and saturated, respectively. The voltage recovery test was accomplished at 220 V; therefore, the reactance determined by this test was a saturated value (Figure 15).

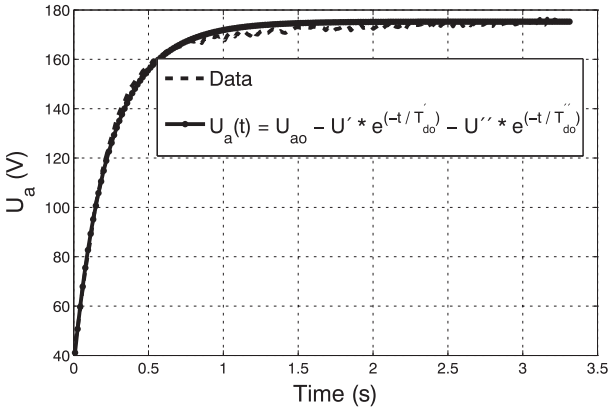

FIGURE 15 Comparison of Data and Voltage Equation of Voltage Recovery Test

The results show some differences in the parameters estimated by different *offline* tests, especially in X_{ds}, which was expected, because all *offline* tests were carried out under different saturation conditions. Some differences were also found in time constants $T_{do}^{'}$ and $T_{do}^{''}$ from tests of SCC and opening of short circuit. The main reason is the difficulty to define the starting point of the subtransient and transient components of the current and voltage. Furthermore, the tested machine has very small time constants that are hard to be determined with accuracy.

The parameters denoted by symbol * were selected from all the *offline* tests to be used as a comparison with trajectory sensitivity method. Those parameters were chosen because the tests were executed at rated voltage.

4 | A COMPARATIVE BETWEEN TRAJECTORY SENSITIVITY AND OFFLINE METHODS

Table 4 shows a comparison between the parameters identified by *offline* and trajectory sensitivity methods.

TABLE 4 Comparison of the Parameters Identified in Per Unit by Offline and Online Methods

Parameters	Offline methods	Trajectory sensitivity method
X_{ds}	0.960	1.09
$X_d^{'}$	0.360	0.49
$X_d^{''}$	0.230	
X_{qs}	0.560	0.574
$T_{do}^{'}$(s)	0.286	0.248
$T_{do}^{''}$(s)	0.185	

20507038, 2017, 2, Downloaded from https://onlinelibrary.wiley.com/doi/10.1002/etep.2255 by Univ of Sao Paulo - Brazil, Wiley Online Library on [10/01/2023]. See the Terms and Conditions (https://onlinelibrary.wiley.com/terms-and-conditions) on Wiley Online Library for rules of use; OA articles are governed by the applicable Creative Commons License

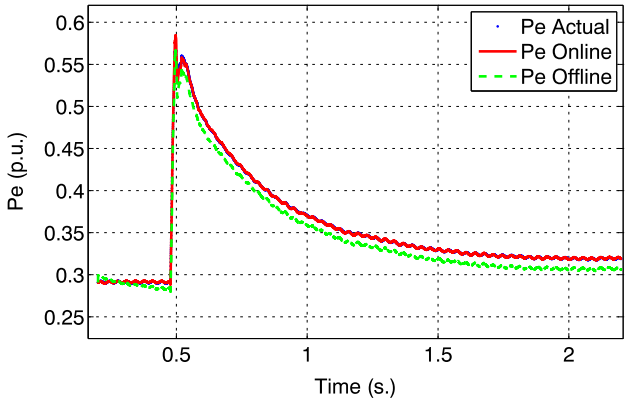

FIGURE 16 Active Power From Actual Measurement Simulated by Online Parameters and Simulated by Offline Parameters

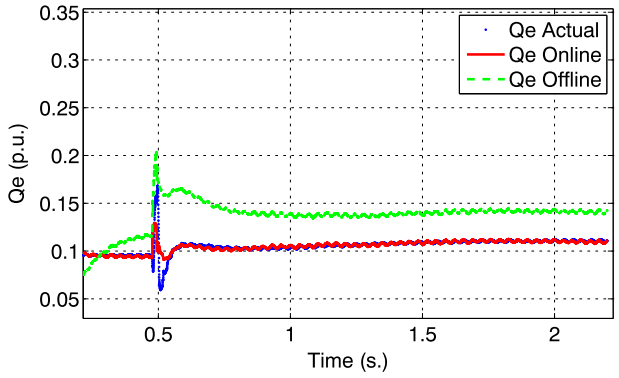

FIGURE 17 Reactive Power From Actual Measurement Simulated by Online Parameters and Simulated by Offline Parameters

The main difference were in X_{ds} and $X_d^{'}$. It might be explained because the results of *offline* methods do not consider the operation point used by trajectory sensitivity method.

Figures 16 and 17 compare the active and reactive power from actual measurements, simulated using parameter obtained by trajectory sensitivity method *(online test)* and obtained by *offline* tests (selected parameters). The figures show that the parameters of trajectory sensitivity method are more confident compared with *offline* tests.

5 | CONCLUSIONS

In this research a comparison between trajectory sensitivity and *offline* methods was accomplished to estimate the parameter of a synchronous generator. Among the *offline* methods the steady-state, SCC, and voltage recovery tests were selected. The tests were executed in a 2-kVA salient pole synchronous generator in a small power system designed in laboratory. The results show some differences in the parameters determined among the different *offline* tests due to mainly different operation condition executed by the tests. The parameter obtained by trajectory sensitivity method yields results more successfully than offline methods because trajectory sensitivity method did not required the disconnection of the generator of the grid. A comparative among the real measurements, simulated using parameter obtained by trajectory sensitivity method and obtained by *offline* tests, showed that the parameters obtained by trajectory sensitivity method are more reliable than those of *offline* method.

6 | LIST OF SYMBOLS AND ABBREVIATIONS

SYMBOLS

I_d, I_q	*d*-axis and *q*-axis stator currents
I, V_T	current and voltage in the generator bus terminal
I_a, U_{an}	armature current and voltage
U_{ae}	armature voltage in generator air-gap line.
V_f, I_f	field voltage and current
E_{fd}	excitation voltage observed in armature winding in per unit
I_{ss}	short circuit current in steady state
$E_q^{'}$	*q*-axis transient voltage
P_e, Q_e	active and reactive power
β	load angle
ω	rotor speed
X_d, X_q	*d*-axis and *q*-axis synchronous reactances
X_{ds}, X_{qs}	*d*-axis and *q*-axis saturated synchronous reactances
X_{du}, X_{qu}	*d*-axis and *q*-axis unsaturated synchronous reactances
$X_d^{'}$, $X_q^{'}$	*d*-axis and *q*-axis transient reactances
$X_d^{''}$	*d*-axis subtransient reactance
$T_d^{'}$, $T_d^{''}$	*d*-axis transient and subtransient short circuit time constant
$T_{do}^{'}$, $T_{do}^{''}$	*d*-axis transient and subtransient open circuit time constant

ABBREVIATIONS

MLC	maximum lagging current
NLSC	no-load saturation curve
SCC	short circuit characteristic

ACKNOWLEDGEMENTS

This research was supported by FAPESP (Fundacao de Amparo a pesquisa de Sao Paulo) under grant 2014/04037-9.

REFERENCES

1. Chowdhury MM, Haque ME, Das D, Gargoom A, Negnevitsky M. "Modeling, parameter measurement and sensorless speed estimation of IPM synchronous generator for direct drive variable speed wind turbine application". *Int. Trans. Electr. Energ. Syst.* 2015;25:1814–1830. doi: 10.1002/etep.1933
2. Kim JM, Moon SI. "A study on a new AVR parameter tuning concept using on-line measured data with the real-time simulator". *Euro. Trans. Electr. Power.* 2006;16:235–246. doi: 10.1002/etep.82

20507038, 2017, 2, Downloaded from https://onlinelibrary.wiley.com/doi/10.1002/etep.2255 by Univ of Sao Paulo - Brazil, Wiley Online Library on [10/01/2023]. See the Terms and Conditions (https://onlinelibrary.wiley.com/terms-and-conditions) on Wiley Online Library for rules of use; OA articles are governed by the applicable Creative Commons License

3. Laroche E, Durieu C, Louis JP. "Parameter estimation accuracy analysis for induction motors". *Euro. Trans. Electr. Power*. 2005;15:123–139. doi: 10.1002/etep.43
4. Torrent M. "Estimation of equivalent circuits for induction motors in steady state including mechanical and stray load losses". *Euro. Trans. Electr. Power*. 2012;22:989–1015. doi: 10.1002/etep.621
5. Zheng J, Wang X, Zhu S. "A novel real-time load modeling method for fast large-disturbance and short-term voltage stability analysis". *Int. Trans. Electr. Energ. Syst*. 2013;23:1373–1395. doi: 10.1002/etep.1666
6. Cari, E.P.T.; Alberto, L.F.C.; de Oliveira, F.M., "Trajectory sensitivity and genetic algorithm based-method for load identification," in Industrial Electronics Society, IECON 2014 - 40th Annual Conference of the IEEE , vol., no., pp.309–314, Oct. 29 2014-Nov. 1 2014. DOI: 10.1109/IECON.2014.7048516
7. Kundur P. *Power System Stability and Control*. New York: McGraw-Hill;1994.
8. Kamwa I, Pilote M, Viarouge P, Mpanda-Mabwe B, Crappe M, Mahfoudi R. "Experience with computer-aided graphical analysis of sudden-short-circuit oscillograms of large synchronous machines,". *IEEE Transactions on Energy Conversion*. Sep 1995;10(3):407–414. doi: 10.1109/60.464861
9. IEEE Guide: Test Procedures for Synchronous Machines Part I--Acceptance and Performance Testing Part II-Test Procedures and Parameter Determination for Dynamic Analysis, in IEEE Std 115–1995 , vol., no., pp.1–198, April 12 1996 doi: 10.1109/IEEESTD.1996.7328817
10. Burth M, Verghese GC, Velez RM. Subset selection for improved parameter estimation in on-line identification of a synchronous generator. *IEEE Transaction on Power and Systems*. February 1999;14(1):218–225. doi: 10.1109/59.744536
11. Cari EPT, Alberto LFC. "Parameter estimation of synchronous generators from different types of disturbances", IEEE Power Energy Society General Meeting, 2011, Detroit, Michigan USA. The electrification of Transportation & The Grid of the Future. IEEE. 2011. doi: 10.1109/PES.2011.6039592
12. Karrari M, Malik OP. "Identification of physical parameters of a synchronous Generator from online measurements,". *IEEE Transactions on Energy Conversion*. June 2004;19(2):407–415. doi: 10.1109/TEC.2003.822296
13. Kyriakides, E.; Heydt, G. T.; Vittal, V.; "On-line estimation of synchronous Generator parameters using a damper current observer and a graphic user interface," in IEEE Transactions on Energy Conversion, vol. 19, no. 3, pp. 499–507, Sept. 2004. doi: 10.1109/TEC.2004.832057
14. Shafighi A, Chahkandi H, Jahani R, Fazli M, Shayanfar HA. "ANN observer for on-line estimation of synchronous generator dynamic parameters," Communication Software and Networks (ICCSN), 2011 IEEE 3rd International Conference on, Xi'an. 2011;674–677. doi: 10.1109/ICCSN.2011.6014179
15. Shariati O, Mohd Zin AA, Khairuddin A, Pesaran HAM, Aghamohammadi MR. "Application of neural network observer for on-line estimation of solid-rotor synchronous generators' dynamic parameters using the operating data," Power and Energy (PECon), 2012 IEEE International Conference on, Kota Kinabalu. 2012;493–498.
16. Dehghani, M.; Nikravesh, S. K. Y.; "Nonlinear state space model identification of synchronous generators", *Electric Power Systems Research*, Volume 78, Issue 5, May 2008, Pages 926–940, ISSN 0378–7796. doi.org/10.1016/j.epsr.2007.07.001.
17. Karayaka HB, Keyhani A, Heydt GT, Agrawal BL, Selin DA. "Synchronous generator model identification and parameter estimation from operating data,". *IEEE Transactions on Energy Conversion*. Mar 2003;18(1):121–126. doi: 10.1109/TEC.2002.808347
18. E. P. T. Cari and L. F. C. Alberto, "Parameter estimation of synchronous generators from different types of disturbances," Power and Energy Society General Meeting, 2011 IEEE, San Diego, CA, 2011, pp. 1–7. doi: 10.1109/PES.2011.6039592
19. Hiskens, I. A.; "Nonlinear dynamic model evaluation from disturbance measurements," in *IEEE Power Engineering Review*, vol. 21, no. 10, pp. 60–60, Oct. 2001. doi: 10.1109/MPER.2001.4311089
20. Tang L, McCalley J. "Trajectory sensitivities: applications in power systems and estimation accuracy refinement," Power and Energy Society General Meeting (PES), 2013 IEEE, Vancouver, BC. 2013;1–5. doi: 10.1109/PESMG.2013.6672533

How to cite this article: Beordo L, Cari EPT, Landgraf TG, Alberto LFC. A Comparative Validation of a Synchronous Generator by Trajectory Sensitivity and Offline Methods. *Int Trans Electr Energ Syst.* 2017;27:e2255. https://doi.org/10.1002/etep.2255

APPENDIX

A.1 | Procedure to calculate time constants and reactances by short circuit test

After the acquisition of short circuit currents, maximum and minimum points in the current waves are obtained from the acquired data, and an average curve is calculated by equation

$$I_{envelope} = \frac{(I_{\max} - I_{\min})}{2} \tag{A.1}$$

This procedure cancels the direct current component present in the envelopes. The analysis of the envelope curve revealed 3 well-defined periods: a short initial one, called subtransient state, in which the current decays quickly; a longer subsequent period, called transient state; and a permanent period, called steady-state. Time constants are associated with the decay tax for the current in subtransient and transient states, ie, 0.368 of its initial value.

The enveloped average curve is guided by equation (A.2), where the first term represents the current in steady-state (I_{ss}); the second represents transient current $i^{'}(t)$, which decays at a time constant $T_d^{'}$; and the third is subtransient current $i^{''}(t)$, which decays at a time constant $T_d^{''}$.

$$i_s(t) = I_{ss} + I^{'} e^{\left(-t/T_d^{'}\right)} + I^{''} e^{\left(-t/T_d^{''}\right)} \tag{A.2}$$

After I_{ss} has been calculated, the direct-axis reactance (X_d) can be determined by

$$X_d = \frac{U}{I_{ss}} \tag{A.3}$$

where U is the armature voltage prior to the short circuit. Current value I_{ss} is then subtracted from $i_s(t)$ and leaves only the component of the transient and subtransient currents.

$$i_s(t) - I_{ss} = I^{'} e^{\left(-t/T_d^{'}\right)} + I^{''} e^{\left(-t/T_d^{''}\right)} \tag{A.5}$$

A semilogarithmic scale is applied to this result, as shown in Figure A1. T_1 is the time at which the curve becomes a straight line, T_2 is the time at which the current reaches the steady state, and from T_1 to T_2, only one transitory current component will exist, because the steady-state component

20507038, 2017, 2, Downloaded from https://onlinelibrary.wiley.com/doi/10.1002/etep.2255 by Univ of Sao Paulo - Brazil, Wiley Online Library on [10/01/2023]. See the Terms and Conditions (https://onlinelibrary.wiley.com/terms-and-conditions) on Wiley Online Library for rules of use; OA articles are governed by the applicable Creative Commons License

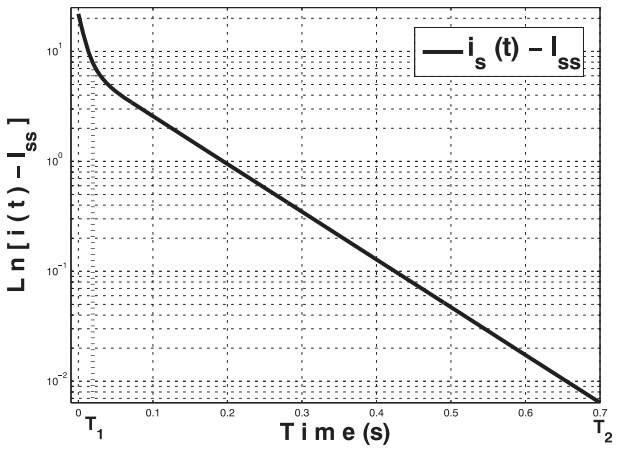

FIGURE A1 Semi-logarithmic scale for the determination of $T_1$and T_2

has been removed and the contribution of the subtransient current is neglected.

From T_1 to T_2, the average enveloped curve is represented by

$$i_s(t) - I_{ss} = I' e^{\left(-t/T'_d\right)} \tag{A.6}$$

The application of the logarithmic function to the period points in the T_1 to T_2 interval results in

$$\ln[i(t) - I_{ss}] = \ln\left[I'\right] - t/T'_d \tag{A.7}$$

which is the equation of a line $y_{tran} = a_1 - b_1 t$, where coefficients a_1 and b_1 are obtained from linear regression, b_1 is the inverse of T'_d ($T'_d = 1/b_1$) and constant I' is calculated from a_1, as $I' = e^{a}{}_1$. The direct-axis transient reactance is determined by

$$X'_d = \frac{U}{A} \tag{A.8}$$

where $A = I_{ss} + i'(0) = I_{ss} + I'$.

The subtransient component can be found from (A.2) by

$$i_s(t) - I_{ss} - I' e^{\left(-t/T'_d\right)} = I'' e^{\left(-t/T''_d\right)} \tag{A.9}$$

The application of the logarithmic function to equation (A.9) yields

$$\ln\left[i_s(t) - I_{ss} - I' e^{\left(-t/T'_d\right)}\right] = \ln[I''] - \frac{t}{T''_d} \tag{A.10}$$

$$\text{or } y_{sub} = a_2 - b_2 t$$

Where $T''_d = (1/b_2)$ and $I'' = e^{a}{}_2$. The direct-axis subtransient reactance is calculated by

$$X''_d = \frac{U}{B} \tag{A.11}$$

where $B = I_{ss} + i'(0) + i''(0) = I_{ss} + I' + I''$.

B.1 | Procedure to calculate the time constants and reactances by voltage recovery test

After the acquisition of voltage the voltage peaks of each phase must be stored after the opening of short circuit, and an average envelop must be determined by equation (B.1). The average curve of the voltage also revealed three periods, namely, steady-state, transient state, and subtransient periods,

$$U(t) = U_{ao} - U' e^{\left(-\frac{t}{T'_{do}}\right)} - U'' e^{\left(-\frac{t}{T''_{do}}\right)} \tag{B.1}$$

where U_{ao} is the steady-state voltage. The procedure is very similar to the sudden short circuit test.

The curve representing the transient and subtransient periods is obtained by

$$U_{ao} - U(t) = U' e^{\left(-t/T'_{do}\right)} + U'' e^{-t/T''_{do}} \tag{B.2}$$

After some cycles, T''_{do} is too short; therefore, a subtransient component can be neglected in this equation. If a logarithmic function is applied to (B.2), this curve becomes a straight line

$$\ln[U_{ao} - v(t)] = \ln[U'] - t/T'_{do} \tag{B.3}$$

$$\text{or } y_{trans} = a_3 - b_3 t$$

where b_3 represents the inverse of constant T'_{do} (or $T'_{do} = 1/b_3$) and constant U' is calculated through coefficient a_3, where $U' = e^{a}{}_3$.

The subtransient component can be found by the subtraction of the contribution of the transient period of equation (B.3)

$$U_{ao} - U(t) - U' e^{\left(-t/T'_{do}\right)} = U'' e^{\left(-t/T''_{do}\right)} \tag{B.4}$$

If a logarithmic function is applied to (B.5), this curve becomes a straight line and results in

$$\ln\left[U_{ao} - U(t) - U' e^{\left(-t/T'_{do}\right)}\right] = \ln[U''] - t/T''_{do} \tag{B.5}$$

$$\text{or } y_{sub} = a_4 + b_4 t$$

where $T''_{do} = (1/b_4)$ and $U'' = e^{a}{}_4$. The reactance values are determined by

$$X_d = \frac{U_{ao}}{I_{sc}} \tag{B.6}$$

$$X'_d = \frac{U_{ao} - U'}{I_{sc}}$$

$$X''_d = \frac{U_{ao} - U' - U''}{I_{sc}}$$

where $U_{ao}$is the voltage in the steady state and I_{sc} is the armature current prior to the opening of the short circuit.

20507038, 2017, 2, Downloaded from https://onlinelibrary.wiley.com/doi/10.1002/etep.2255 by Univ of Sao Paulo - Brazil, Wiley Online Library on [10/01/2023]. See the Terms and Conditions (https://onlinelibrary.wiley.com/terms-and-conditions) on Wiley Online Library for rules of use; OA articles are governed by the applicable Creative Commons License